JOURNAL OF MATERIALS SCIENCE 29 (1994) 6397–6402

Auger electron spectroscopic analysis of chemical vapour deposited diamond/substrate interfaces

Q. S. CHIA, C. M. YOUNES*, P. G. PARTRIDGE*, G. C. ALLEN*,
P. W. MAY‡, C. A. REGO‡
*H.H. Wills Physics Laboratory, * Interface Analysis Centre, and ‡ School of Chemistry, University of Bristol, Bristol, UK*

Auger electron spectroscopy has been used to identify the allotropes of carbon in chemical vapour deposited diamond films deposited on copper and tungsten wires and on SiC and silica fibres and to measure the thickness and composition of the diamond/substrate reaction layers. The significance of these results for the manufacture of diamond fibres is discussed.

1. Introduction

The growth of diamond thin films produced by chemical vapour deposition (CVD) on non-diamond substrates has been studied extensively over the last five years [1, 2]. Recently, diamond fibres have been produced by CVD on ceramic and carbon-fibres and metal wire cores [3]. This has led to the possibility of exploiting the properties of diamond on a large scale by means of diamond fibre composites [3, 4]. However, the properties of the composites will depend on the chemical nature and the microstructure of the interface between the core and the diamond coating. This will depend on reactions between the substrate and hot gases during deposition and on diamond nucleation and growth mechanisms.

Diamond films are currently grown by various methods (r.f. plasma-enhanced CVD [5], microwave plasma-enhanced CVD [6–8], and hot filament-enhanced CVD [9, 10]) on a variety of planar substrates including silicon, SiO_2, SiC, platinum, gold, copper, molybdenum, titanium and tungsten. Relatively little work, however, has been reported for diamond growth on small-diameter fibres and wires [3]. These studies have used mostly scanning electron microscopy, Raman spectroscopy and X-ray diffraction to characterize the surface morphology and phases present. More recently, high-resolution analytical techniques such as transmission electron microscopy (TEM) and Auger electron spectroscopy (AES) have been used to characterize diamond films and diamond film/substrate interfaces [11–13].

As part of an investigation into the properties of CVD diamond fibres, SEM and AES techniques were used to study the effect of various fibre cores on the morphology and nucleation of the diamond film and to obtain the chemical composition and thickness of the reaction layers at the diamond/substrate interfaces. The results obtained are described.

2. Experimental procedure

A standard hot-filament CVD reactor was used to deposit diamond, with a gas mixture of 1% methane in hydrogen, a gas flow rate of 200 standard $cm^3 min^{-1}$ and a chamber pressure of 30 torr (1 torr = 133.322 Pa). The gases were dissociated either by a 11 mm long, 8 mm diameter vertical helical tantalum wire filament heated electrically to 2000 °C (Fig. 1a) or by a horizontal 11 mm long, 3 mm diameter filament (Fig. 1b) [2].

Substrates were 200 μm diameter tungsten wire, 100 μm diameter copper wire, 60 μm diameter hollow silica fibre, and 140 μm diameter Textron SCS-6 SiC fibre. All specimens were manually abraded with 3 μm diameter diamond grit to enhance diamond nucleation and cleaned in methanol. Each tungsten specimen was mounted co-axially inside the vertical filament (Fig. 1a). The other specimens were mounted horizontally outside and about 3–4 mm below the filament and just above a 150 W light bulb (Fig. 1b), which led to a more uniform diamond coating. The temperature of the substrate was maintained at 900 °C and the average diamond deposition rate was 0.65 $\mu m\, h^{-1}$ (Fig. 2).

The diamond-coated specimens were fractured in air, through the diamond-coated area, into two equal lengths and mounted by pressing into indium foil before loading into the chamber of the Auger spectrometer.

AES analysis was performed with a Perkin–Elmer PHI 595 scanning Auger microprobe equipped with a double-pass cylindrical analyser. The electron gun operated at 3 keV with a beam current of 70 nA and a beam diameter of ~ 0.3 μm. Sputter cleaning was carried out using an argon ion gun at a sputter rate of 40 $nm\, min^{-1}$. The Auger spectrometer chamber was maintained at a base pressure of $< 10^{-9}$ torr during imaging and analysis.

0022–2461

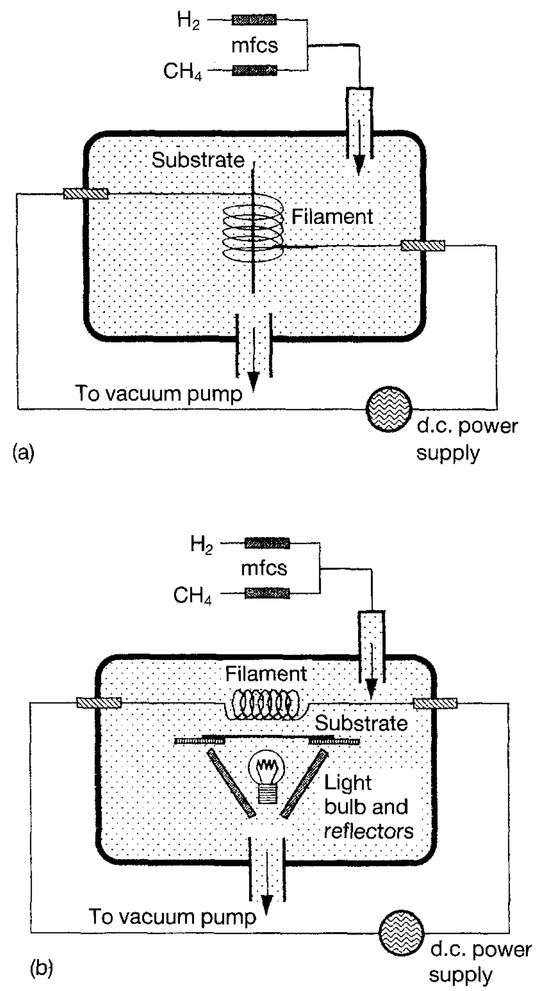

Figure 1 Schematic diagrams of chemical vapour deposition technique for diamond fibres. mfc: mass flow controller. Fibre substrate mounted: (a) coaxially within filament; (b) outside the filament.

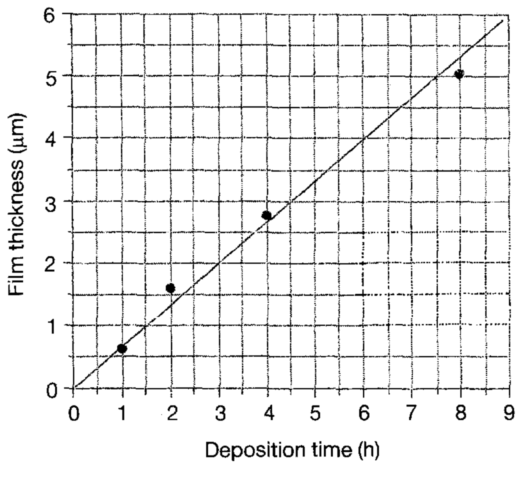

Figure 2 Diamond film thickness versus deposition time for diamond grown on tungsten wire. Average growth rate = 0.65 $\mu m\,h^{-1}$.

3. Results

3.1. Deposition on tungsten wire

Coating times were 1, 2, 4 and 8 h. The diamond deposit grew by nucleation and growth of individual crystals. Each crystal showed well-developed three-four-sided facets whose size increased with increasing deposition time. The nucleation density and the deposit thickness and uniformity were dependent on the local temperature and surface morphology. A region of uniform coating after 8 h deposition and a partially coated region after 4 h deposition are shown in Fig. 3a and b respectively. In the latter the rows of crystals were aligned parallel to the scratches and grooves on the tungsten surface. When eventually complete coverage occurred, the film thickness was uniform. This uniformity could only arise from the partially coated state (Fig. 3b) by fresh nuclei growing on the uncoated regions more rapidly than the initial nuclei or by sideways growth at the edges of the existing diamond-coated region. The observations in the present study indicate the latter mechanism operated.

The Auger electron spectra characteristic of the various allotropic forms of carbon are shown in Fig. 4a [14]. Spectra obtained from the surface of the deposit and exposed areas of the substrate indicated that only carbon and oxygen were present, with a much smaller peak intensity for oxygen. Because the latter disappeared after sputtering for about 5 s, it was concluded that it was an adsorbed contamination layer arising from previous exposure to air.

The fine structure of the *K L L* carbon peak (Fig. 4b) was characteristic of natural diamond [14]. Exposed areas between the diamond crystals yielded spectra typical of amorphous carbon (Fig. 4c). The shift in the energy of the diamond peak by about 7 eV towards lower energies compared with the peak for amorphous carbon detected on the same specimen (Fig. 4c) is clearly apparent. The shift in the spectrum for diamond arises mainly from the charging effect on the surface of the less-conductive diamond compared with

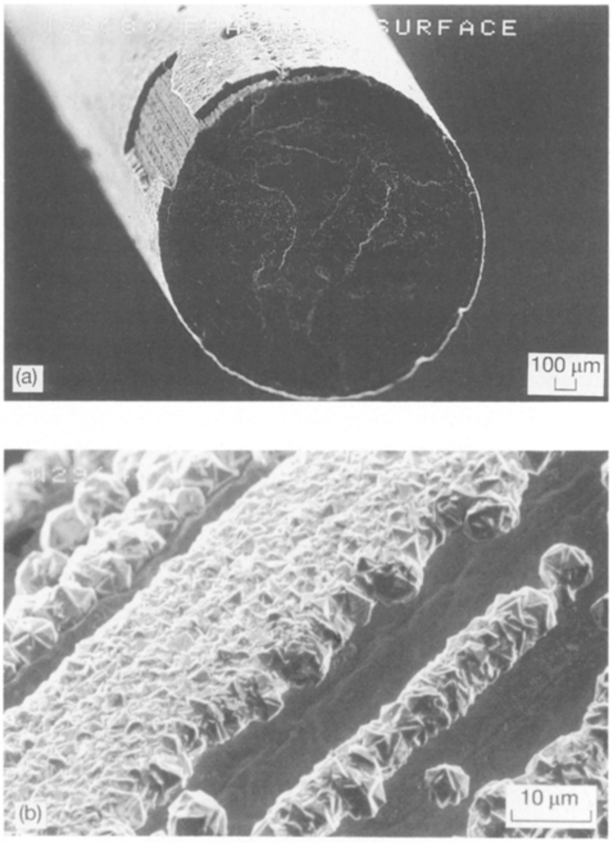

Figure 3 Diamond coating on tungsten wire: (a) fractured fibre; (b) diamond crystals aligned along scratch lines and grooves.

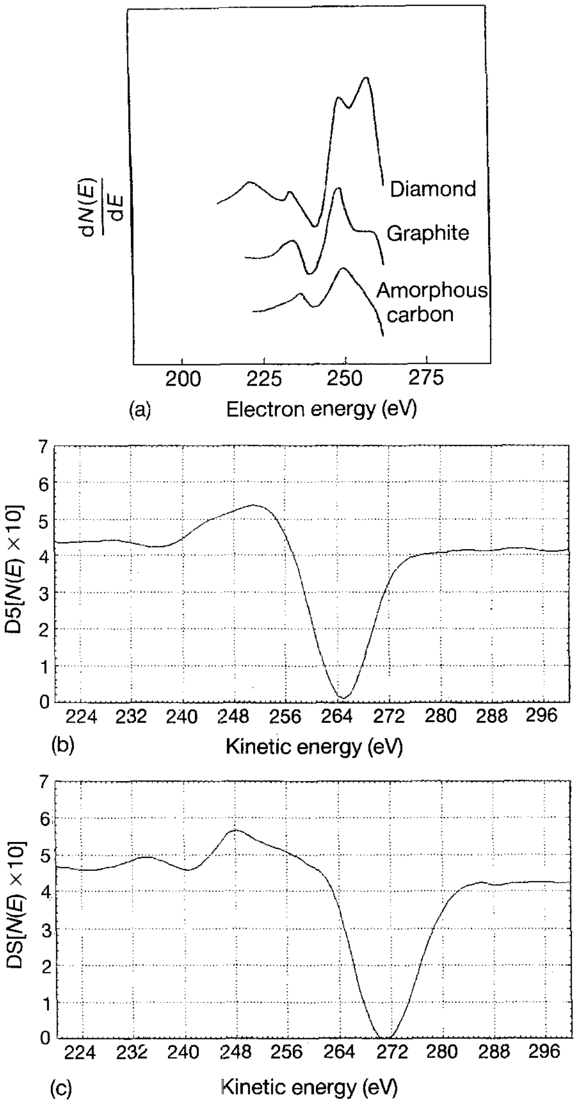

Figure 4 Auger spectra: (a) fine structure of diamond, graphite and amorphous carbon [14]; (b) typical spectrum from diamond crystal on fibre surface; (c) spectrum from exposed areas between crystals indicating amorphous carbon.

amorphous or graphitic carbon. This energy shift was found to be reproducible in the present experiments. Because the binding energy of the core electrons in diamond, graphite and amorphous carbon differ only by less than 1 eV [15], the peak energy shift offers an additional method for detecting carbon allotropes at the surface and in the bulk.

The exposed surfaces between the diamond coating were analysed by sequential AES and argon ion sputtering using specimens coated for various times. After an outermost amorphous carbon layer was first removed by sputtering for 1 min, a tungsten carbide phase was identified from the characteristic Auger line shape for W_2C [16]. The changes in the spectra with increased depth from the carbide layer surface (Fig. 5a) to the base of the carbide layer (Fig. 5c) allowed the thickness of the carbide layer to be determined (Fig. 6). The carbide layer thickness of about 2.5 μm was found to be independent of the deposition time.

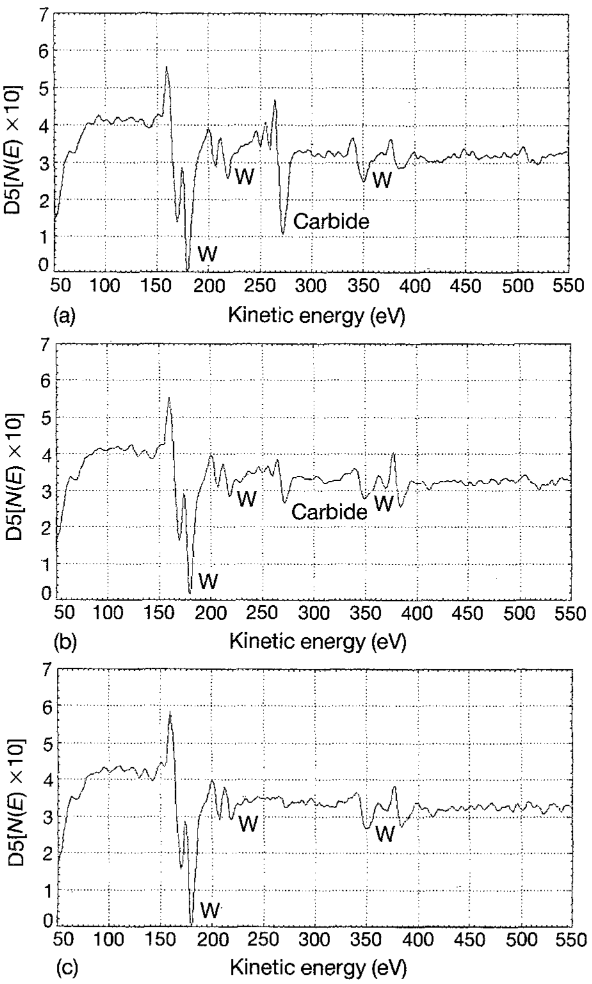

Figure 5 Auger spectra showing progressive decrease in tungsten carbide peak with increasing depth from exposed surface of the wire where diamond had spalled off during fracture: (a) exposed surface after sputter cleaning; (b) after sputter ion milling; (c) at the base of the carbide layer.

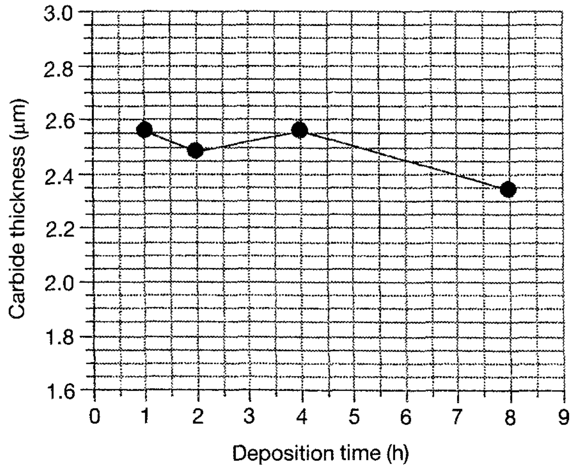

Figure 6 Tungsten carbide layer thickness on tungsten wire versus deposition time, obtained by AES depth profiling.

3.2. Deposition on SiC fibre

The surface of the SCS-6 fibre was smooth with no evidence of abrasion scratches. A deposition time of 6 h produced a typical uniform faceted diamond film on the fibre of about 3.8 μm (Fig. 7a); the surface etch pits visible beneath the coating (Fig. 7b and c) were attributed to attack by the atomic hydrogen during deposition. A close-up of the fracture surface of the diamond film (Fig. 7c) shows the columnar crystal growth structure and the pitted surface. An AES

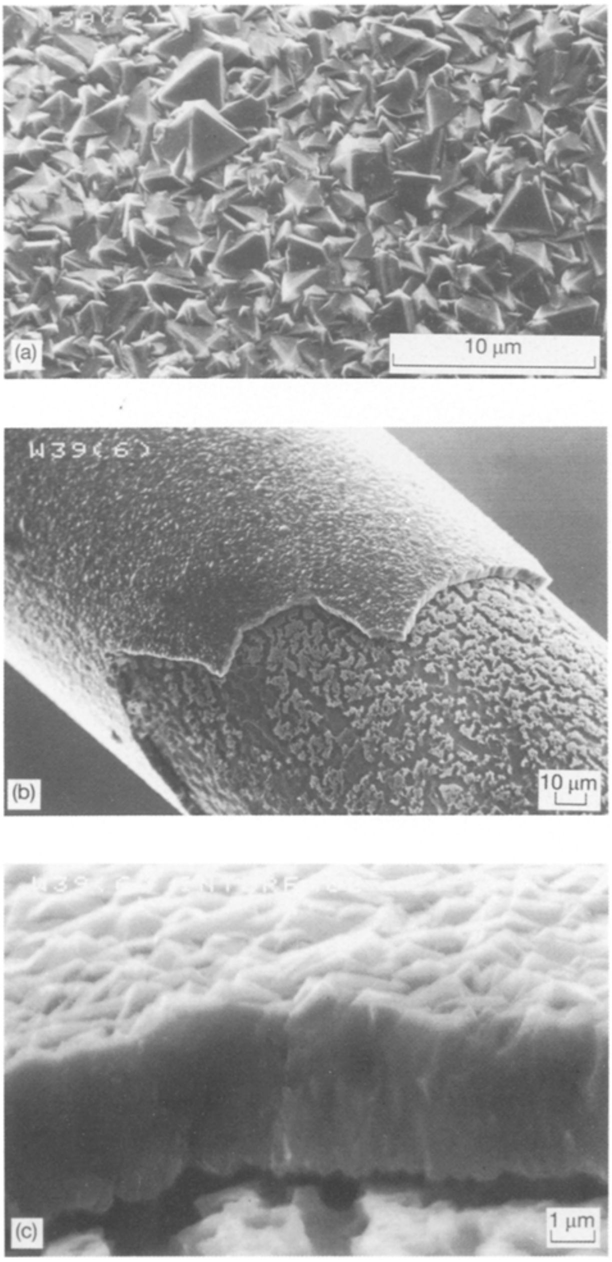

Figure 7 Diamond coating on SiC fibre showing: (a) faceted diamond crystals on the surface; (b) pitted fibre surface below diamond coating; (c) pitted surface and uniform diamond coating.

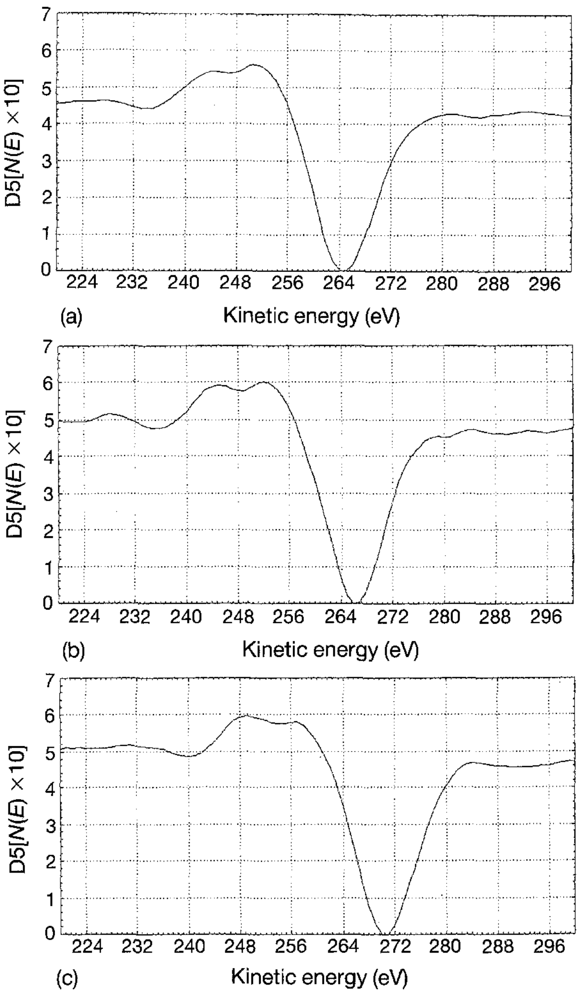

Figure 8 Diamond coating on SiC. Auger spectra showing typical displacement in the carbon peak and change in the shape of the peak with increasing depth: (a) top of diamond coating; (b) at a depth of about two-thirds of the coating thickness; (c) base of coating.

spectrum from such surface areas indicated the presence of silicon and carbon with traces of calcium and oxygen. The concentrations of oxygen were higher than for the tungsten substrate, and on the SiC substrate were always associated with calcium; these species were therefore believed to be associated with the carbonaceous surface layer on this fibre.

The local composition through the thickness of the diamond coating was determined by moving the electron probe on the diamond fracture from the top surface to the substrate surface. The fine structure (shape) of the *K L L* carbon peak and the energy shift in the AES showed a gradual transition from the diamond structure at the surface, with characteristic sp^3 bonding (Fig. 8a), to diamond and traces of graphite at a depth of 2.6 μm (Fig. 8b), and to a graphitic type of carbon sp^2 bonding at the base of the film. These results are consistent with other work on diamond deposited on silicon [13, 17], which indicate the co-deposition of graphite and disordered carbon together with diamond in the early growth stages when the methane concentration was about 1% or higher.

3.3. Deposition on silica fibre

The surface of the SiO_2 fibre contained very fine scratches after abrading. The fibre was difficult to handle without fracture and sometimes fractured during deposition. A uniform diamond coating was obtained, however, similar to that obtained for SiC as shown for a fractured specimen in Fig. 9. The coating thickness was about 4.3 μm and good adhesion was found between the diamond coating and the fibre. The diamond structure of the film was confirmed by AES from the coating surface.

At the diamond/silica interface three distinct phases, SiC, reduced silica and SiO_2, were detected. The identification of these phases in Fig. 10 relies on our calibration for SiC and the characteristic energy shift due to Si–O bonding for SiO_2 and reduced fused silica [18]. It was not possible to determine the exact thickness of the carbide layer because of the charging

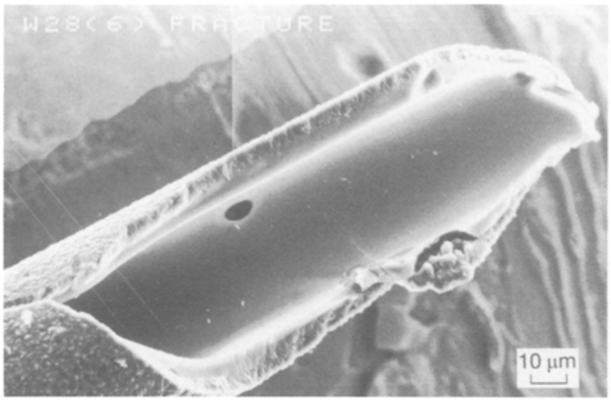

Figure 9 Diamond coating on a hollow silica fibre after fibre fracture.

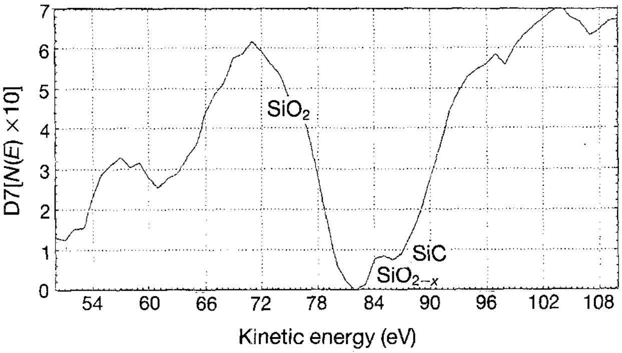

Figure 10 Auger spectrum from the diamond/silica interface.

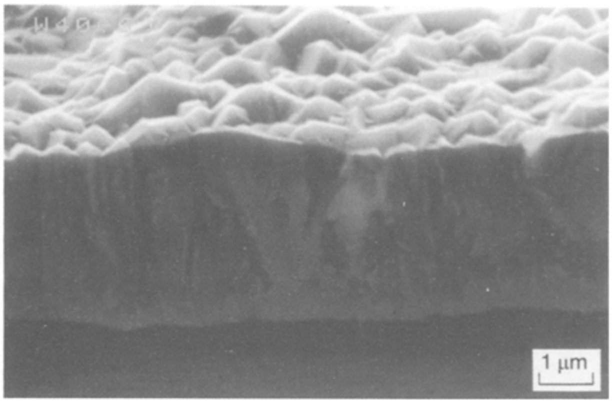

Figure 11 Diamond coating on a copper wire.

effect of the insulating silica. However sputtering for ~ 8 s which removed about 5.5 nm, was always sufficient to expose the substrate matrix, indicating the SiC layer was less than 5 nm. Research elsewhere [19] has confirmed the formation of thin (5–10 nm) intermediate SiC layers between diamond films and silicon substrates. In addition, other studies reported the conversion of SiO_2 to SiC and the evolution of CO [20]. This is consistent with our results that indicate diamond nucleation on silica begins with the formation of SiC.

3.4. Deposition on copper wire

After abrading, fine scratches were visible superimposed on the surface grooves produced during the wire manufacture. After deposition for 6 h, a uniform 3.4 µm thick film (Fig. 11) identified as diamond by AES, was produced similar to that on SiC. Because copper does not react with carbon, no interface layer was detected, but the adhesion between the diamond and the copper was poor.

4. Discussion and conclusions

Our results show that diamond can be grown successfully on various fibre core materials, but reactions at the substrate/diamond interface depend on the type of core. To avoid embrittlement and obtain high interface shear strength, the interface layer thickness should not be too thick. The present study has shown that the tungsten carbide interface layer thickness is independent of deposition time. This suggests that stable carbide reaction layers form during deposition, but before coverage of the substrate surface by diamond is complete. Thus, for a minimum reaction layer thickness, the deposition time is less important than a combination of high diamond nucleation density and high growth rate. The AES technique has been shown to discriminate readily at high spacial resolution between the various allotropes of carbon. This is very useful for indicating the extent of mixed diamond and non-diamond regions in the coating, which may be associated with lower strength and stiffness.

It is known that carbide layers increase the bond strength between diamond and metals, but too thick a reaction layer may lead to embrittlement of the fibre. In this study AES has been used to determine both interface layer thicknesses and composition. The results suggest that SiC may be effective in forming thin thermally stable reaction layers between diamond coatings and substrates. AES therefore provides a valuable tool for relating microstructure to physical and mechanical properties in diamond composite systems.

Acknowledgements

The authors thank Professors M. N. R. Ashfold and J. W. Steeds for supporting this research programme and D. Cherns and J. A. Wilson for their advice and help with the microscopy.

References

1. M. N. R. ASHFOLD, P. W. MAY, C. A. REGO and N. M. EVERITT, *Chem. Soc. Rev.* **23** (1994) 21.
2. P. W. MAY, C. A. REGO, R. M. THOMAS, M. N. R. ASHFORD, K. N. ROSSER, P. G. PARTRIDGE and N. M. EVERITT, in "Proceedings of the 3rd International Symposium on Diamond Materials", Honolulu, May 1993 (Electrochemical Society).
3. P. G. PARTRIDGE, P. W. MAY and M. N. R. ASHFOLD, *Overview, Mater. Sci. Technol.* **10** (1994) 177.
4. P. G. PARTRIDGE, P. W. MAY, M. N. R. ASHFOLD C. A. REGO, *Mater. Sci. Technol.* (1994) in press.
5. S. MATSUMOTO, *J. Mater. Sci. Lett.* **4** (1985) 600.
6. S. SATO, M. KAMO and N. SETAKA, in "High Tech Ceramics", Ed. P. Vincenzi (Elsevier, Amsterdam, 1987).
7. K. KOBASHI, K. NISHIMURA, Y. KAWETI and T. HORIUCHI, *J. Vac. Sci. Technol.* **46** (1988) 1816.

8. C. P. CHANG, D. L. FLIMM, D. E. IBBOSTON and J. A. MUCHA, *J. Appl. Phys.* **63** (1988) 1744.
9. S. J. HARRIS, A. M. WEINER and T. A. PERRY, *Appl. Phys. Lett.* **53** (1985) 1605.
10. S. S. RUSK and J. Y. LEE, *J. Appl. Phys.* **69** (1991) 2618.
11. B. E. WILLIAMS and J. J. GLASS, *J. Mater. Res.* **4** (1989) 373.
12. D. J. PICKRELL, W. ZHU, A. R. BIRZIAN, R. E. NEWNHAM and R. MESSIER, *J. Mater. Res.* **6** (1991) 1264.
13. P. J. FALLON and L. M. BROWN, *Diamond Rel. Mater.* **2** (1993) 1004.
14. P. G. LURIE and J. M. WILSON, *Surface Sci.* **65** (1977) 476.
15. F. R. McFEELY, S. P. KOWALCZYK, L. LEY, R. G. CAVELL, R. A. POLLAK and D. A. SHIRLEY, *Phys. Rev. B* **9** (1974) 5268.
16. P. E. PEHRSSON and D. RAMAKER, *J. Mater. Res.* **8** (1993) 2716.
17. W. ZHU, C. A. RANDALL, A. R. BADZIAN and R. MESSIER, *J. Vac. Sci. Technol.* **7** (1993) 2315.
18. H. H. MADDEN, *ibid.* **18** (1981) 677.
19. B. R. STONER, G. H. M. MA, S. D. WOLTER and J. T. GLASS, *Phys. Rev. B* **45** (1992) 11067.
20. X. K. CHEN, G. MATUA, S. PRAMANICK and J. NARAYAN, in "2nd International Symposium on Diamond Materials", Vol. 8 (1991) p. 91.

Received 28 April
and accepted 7 June 1994